

Measurement of spin diffusion length in sputtered Ni films using a special exchange-biased spin valve geometry

Charles E. Moreau^{a)}

Department of Physics, Albion College, Albion, Michigan 49224

Ion C. Moraru, Norman O. Birge, and William P. Pratt, Jr.

Department of Physics and Astronomy, Michigan State University, East Lansing, Michigan 48824-2320

(Received 13 September 2006; accepted 21 November 2006; published online 2 January 2007)

The authors report the spin diffusion length at 4.2 K in sputtered Ni of $l_{sf}^{Ni}=21\pm 2$ nm, and spin-dependent scattering parameters in Ni and at Ni/Cu interfaces. They have employed current perpendicular to plane giant magnetoresistance in both a traditional and an alternative exchange-biased spin valve geometry that inserts a Ni “spoiler” layer into a Py/Cu/Py spin valve. Fits to data of $A\Delta R$ vs Ni thickness using Valet-Fert theory [Phys. Rev. B **48**, 7099 (1993)] show good agreement between fit parameters for both sample geometries. © 2007 American Institute of Physics. [DOI: 10.1063/1.2424437]

The distance over which an electron retains memory of its spin direction while propagating through a metal has been of interest ever since the pioneering spin injection experiments of Johnson and Silsbee.¹ In the context of ferromagnetic/nonmagnetic (F/N) multilayers or spin valves, the size of the giant magnetoresistance² (GMR) signal depends not only on the spin scattering asymmetries of the F metal and of the F/N interface, but also on the spin diffusion lengths of both metals.³ More recently, there has been intense interest in the properties of hybrid ferromagnetic/superconductor (F/S) systems. Both the critical current through a S/F/S Josephson junction,⁴ and the propagation of superconducting order of spin-triplet symmetry in a S/F bilayer⁵ are limited by the spin diffusion length in the F metal.

Several measurements of the spin diffusion length l_{sf} of F and N metals have been made previously. In general, the values of l_{sf} found in ferromagnetic alloys such as Permalloy⁶ or Co₉₁Fe₉ (Ref. 7) are considerably smaller than those found in elemental ferromagnets, such as Co.⁸ This fact motivated our use of the “pure” ferromagnet Ni in recent work on the F/S system Ni/Nb,⁹ and also motivates the present measurements of l_{sf} in our sputtered Ni films.

Our first approach to measuring l_{sf} in Ni is to make exchange-biased spin valves of the form Cu(10)/FeMn(8)/Py(8)/Cu(15)/Ni(d_{Ni})/Cu(10)/FeMn(2)/Cu(5), where all thickness are specified in nanometer. In these samples Ni is the “free” F layer and Permalloy (Py = Ni₈₄Fe₁₆) is the “pinned” F layer, whose magnetization is fixed by exchange-biased coupling to the adjacent Fe₅₀Mn₅₀ antiferromagnetic layer. For such a spin valve, application of a modest in-plane magnetic field can change the magnetization of the free layer without disturbing that of the pinned layer, thereby producing antiparallel (AP) and parallel (P) relative magnetization states. For the current direction perpendicular to the planes (CPP), the specific resistance is AR (sample cross-sectional area times CPP resistance), and the specific magnetoresistance is $A\Delta R=A(R^{AP}-R^P)$. When the

thickness of the Ni layer d_{Ni} is much less than l_{sf}^{Ni} , the simple two-current series-resistor¹⁰ model gives

$$A\Delta R \propto \beta_{Ni}\rho_{Ni}^*d_{Ni} + 2\gamma_{Ni/Cu}AR_{Ni/Cu}^* \quad (1)$$

When $d_{Ni} \gg l_{sf}^{Ni}$,

$$A\Delta R \propto \beta_{Ni}\rho_{Ni}^*l_{sf}^{Ni} + \gamma_{Ni/Cu}AR_{Ni/Cu}^* \quad (2)$$

Thus, a plot of $A\Delta R$ vs d_{Ni} will be linear at small values of the Ni thickness and saturate at large values. Valet-Fert³ (VF) theory interpolates between these two limiting cases, and the crossover between the two behaviors can be used to extract l_{sf}^{Ni} . In Eqs. (1) and (2), β_{Ni} is the bulk spin-scattering asymmetry, $\rho_{Ni}^* = \rho_{Ni}/(1-\beta_{Ni}^2)$, ρ_{Ni} is the normal resistivity of Ni, $\gamma_{Ni/Cu}$ is the interface spin-scattering asymmetry, $AR_{Ni/Cu}^* = AR_{Ni/Cu}/(1-\gamma_{Ni/Cu}^2)$, and $AR_{Ni/Cu}$ is the interface resistance of the Ni/Cu interface.

Our sample design and preparation by sputtering are described in detail elsewhere.¹¹ We only note here that the sample is sandwiched between two ~1-mm-wide superconducting Nb cross strips and measured at 4.2 K. The 2 nm FeMn layer was added to disrupt spin memory before reaching the superconducting Nb contact, thereby enhancing $A\Delta R$.

Figure 1 shows both the raw GMR signal (inset) and a plot of $A\Delta R$ vs d_{Ni} , as d_{Ni} was varied over the range of 5–40 nm.¹² The data show the expected behavior with $A\Delta R$ first increasing and then saturating as d_{Ni} increases. However, the overall value of $A\Delta R$ and the change in $A\Delta R$ with d_{Ni} are small, because of relatively small $\gamma_{Ni/Cu}AR_{Ni/Cu}^*$ and $\beta_{Ni}\rho_{Ni}^*$, respectively.

The solid black curve in Fig. 1 represents a best fit to the data using a numerical solution of VF theory. This fit uses three free parameters $l_{sf}^{Ni}=21\pm 2$ nm, $\beta_{Ni}=0.14\pm 0.02$, and $\gamma_{Ni/Cu}=0.29\pm 0.05$. This last value is consistent with the value $\gamma_{Ni/Cu}=0.25$ calculated by Stiles and Penn¹⁴ for the Ni/Cu (111) interface. Additionally, we use $AR_{Ni/Cu}^*=0.18\pm 0.03$ f Ω m², determined by multilayer measurements (see below), and $\rho_{Ni}=33\pm 3$ n Ω m measured in-plane on a separate $d_{Ni}=200$ nm film. An earlier CPP measurement of ρ_{Ni} is in very good agreement with this value.¹⁵

This method for determining the spin diffusion length relies on the curvature in the data of Fig. 1 caused by the finite l_{sf} . Because the overall change in $A\Delta R$ from d_{Ni}

^{a)}Electronic mail: cmoreau@albion.edu

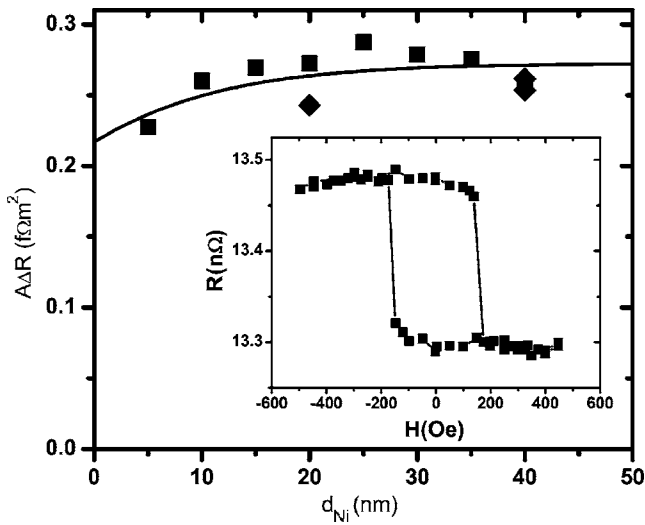


FIG. 1. $A\Delta R$ vs d_{Ni} data for a traditional Py/Cu/Ni exchange-biased spin valve. Data come from two different sample runs. The solid curve represents a best fit using a numerical solution of VF theory with $l_{sf}^{Ni}=21$ nm. Inset shows a typical spin valve signal for this sample geometry.

$=5$ nm to its saturation value is relatively small, we find that our value for l_{sf} above is poorly constrained. That is, the best fit line is somewhat insensitive to the value of l_{sf} if we let the other parameters vary simultaneously. To improve on this requires a sample geometry that provides an overall greater change in the value of $A\Delta R$ as d_{Ni} is increased.

We accomplish this by introducing a different sample geometry whose design produces the desired large change in $A\Delta R$ with d_{Ni} . We take a Py/Cu/Py spin valve where Py has a relatively large β ($\beta_{Py}=0.93\pm 0.07$) (Ref. 6) and insert a Ni layer between the pinned Py layer and the Cu layer. We call this the “spoiler” geometry because, with $\beta_{Ni}\ll\beta_{Py}$, $A\Delta R$ decreases as d_{Ni} increases. For $d_{Ni}>l_{sf}^{Ni}$, VF theory gives approximately

$$A\Delta R(d_{Ni}) - A\Delta R(\infty) \propto e^{-d_{Ni}/l_{sf}^{Ni}}. \quad (3)$$

In the spoiler geometry, we chose Cu(10)/FeMn(8)/Py(8)/Ni(d_{Ni})/Cu(15)/Py(24)/Cu(10). Again one Py layer was pinned by the adjacent layer of FeMn. The second Py layer was left free. The Ni spoiler layer is inserted between the pinned layer and the Cu spacer. Here d_{Ni} was varied from 0 to 50 nm.

Figure 2 shows that in the spoiler geometry $A\Delta R$ decreases rapidly with d_{Ni} and then saturates. Because of the large value of β_{Py} , as $d_{Ni}\rightarrow 0$, $A\Delta R$ is much larger than that in Fig. 1. Additionally, the overall change in $A\Delta R$ with d_{Ni} is many times larger in the spoiler geometry.

The numerical fit using VF theory (solid black curve shown in Fig. 2) was carried out in two steps. (1) The theory was first fitted to the data for $d_{Ni}=0$ by setting $\beta_{Py}=0.78$, within the constraint of its earlier value.⁶ This value of β_{Py} is used in the fits on both Figs. 1 and 2. (2) Next the theory was fitted to the data for $d_{Ni}>2$ nm. This 2 nm minimum value of d_{Ni} is arbitrarily chosen to fall in the region where there are no data points and to simulate a possible incomplete formation of the Ni/Cu interface for $d_{Ni}\leq 2$ nm. In the fit, the values of ρ_{Ni} and $AR_{Ni/Cu}^*$ are fixed as for our fit in Fig. 1. The remaining three parameters, l_{sf}^{Ni} , β_{Ni} , and $\gamma_{Ni/Cu}$, are left free so that a self-consistent set of these parameters is obtained for both Figs. 1 and 2. More importantly, the fit in

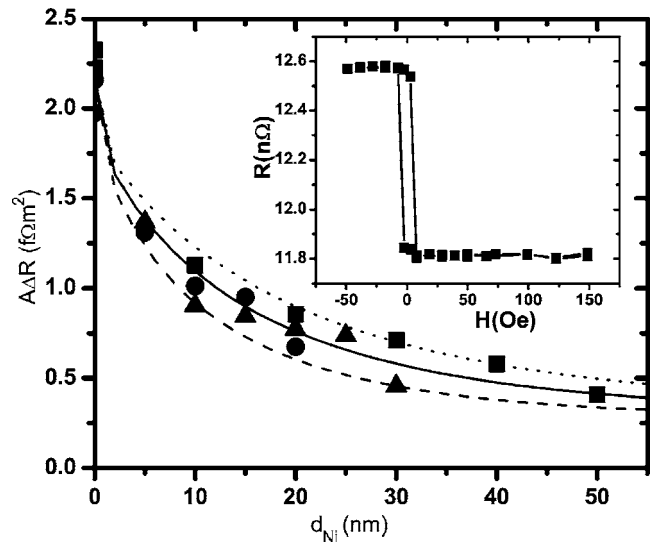


FIG. 2. $A\Delta R$ vs d_{Ni} data for a “spoiler” Py/Ni/Cu/Py exchange-biased spin valve. Data come from three different sample runs. The dotted, solid, and dashed curves are for $l_{sf}^{Ni}=25, 21,$ and 17 nm, respectively. Inset shows a typical spin valve signal for this sample geometry.

Fig. 2 is much more sensitive to the value of l_{sf}^{Ni} , providing a tighter constraint on this parameter. This sensitivity is illustrated by the dotted and dashed curves in Fig. 2 for $l_{sf}^{Ni}=25$ and 17 nm, respectively.

Our measured value of $l_{sf}^{Ni}=21\pm 2$ nm is longer than that typically associated with alloys such as Py ($l_{sf}^{Py}=5.5\pm 1$ nm) (Ref. 6) and $Co_{91}Fe_9$ ($l_{sf}^{CoFe}=12\pm 1$ nm),⁷ but shorter than that reported in Co ($l_{sf}^{Co}\approx 59$ nm).⁸ We expect that the value of l_{sf} is determined by spin-orbit scattering at impurities and defects in our sputtered Ni films.⁸ Our Ni sputtering target is 99.99% pure, with no metallic impurities greater than 0.001%.

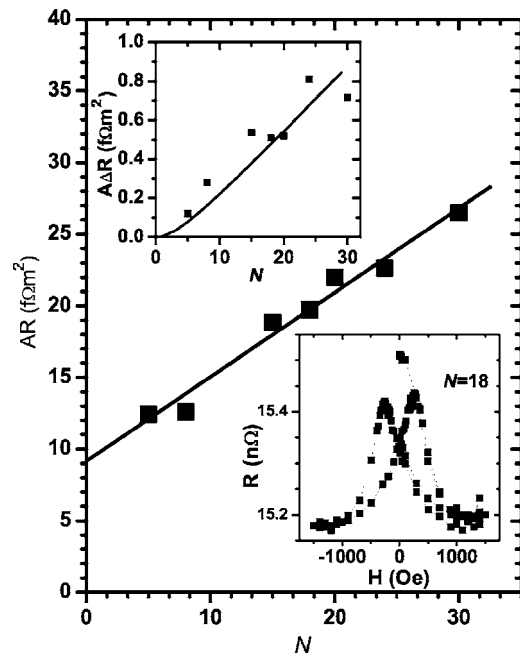


FIG. 3. AR vs number of Ni/Cu repeats (N) for Ni/Cu multilayers. Upper inset: $A\Delta R$ vs N for the Ni/Cu multilayers. The solid line represents the calculation using our values of parameters obtained from the spin valve data. Lower inset: raw GMR data for the sample with $N=18$.

To determine the value of $AR_{\text{Ni/Cu}}^*$ employed in the fits above, we utilized multilayer samples where the total thicknesses of Cu and Ni add to a fixed value (360 nm) in each sample, but the number of multilayer repeats N is increased. Thus $N(d_{\text{Cu}}+d_{\text{Ni}})=360$ nm. Additionally, we fixed the value of $d_{\text{Ni}}=8$ nm. As such, the slope of a plot of AR^{AP} vs N should have a slope of $(\rho_{\text{Ni}}^*-\rho_{\text{Cu}})d_{\text{Ni}}+2AR_{\text{Ni/Cu}}^*$.¹¹ Figure 3 shows the plot of AR^{AP} vs N . The value of AR^{AP} is taken from the virgin state, before any magnetic field has been applied to the sample (see lower inset).¹⁶ Using the slope shown, as well as the values of $\rho_{\text{Cu}}=4.5$ n Ω m and $\rho_{\text{Ni}}=33\pm 3$ n Ω m, yields the value of $AR_{\text{Ni/Cu}}^*=0.18\pm 0.03$ f Ω m² used in the fits above. Our measured value is considerably lower than that calculated by Stiles and Penn,¹⁴ $AR_{\text{Ni/Cu}}^*=0.37$ f Ω m².

As a further check on our fit parameters, we plot in the upper inset to Fig. 3 the GMR signal, ΔR vs N , for the multilayers. The solid line is the prediction of the VF theory based on the parameter values obtained from the fits shown in Figs. 1–3, with no adjustments. The agreement is excellent, which confirms that the virgin state of the multilayer exhibits good AP local alignment.¹⁶

In conclusion, we report the value of the spin diffusion length in Ni and of the spin-dependent scattering parameters in Ni and at Ni/Cu interfaces. We utilize a spin valve geometry which places a “spoiler” layer into the spin valve sandwich. This geometry overcomes the weak spin-scattering asymmetry of Ni and allows for tighter constraints on the fits to the data using Valet-Fert theory.

The authors thank Nick Moroz and Kathy Walsh for performing some of the magnetic measurements, and Reza Loloee for technical assistance. This work was supported by the NSF under Grant Nos. DMR-0405238 and DMR-0501013.

- ¹Mark Johnson and R. H. Silsbee, Phys. Rev. Lett. **55**, 1790 (1985).
- ²M. N. Baibich, J. M. Broto, A. Fert, F. Nguyen Van Dau, F. Petroff, P. Eitenne, G. Creuzet, A. Friederich, and J. Chazelas, Phys. Rev. Lett. **61**, 2472 (1988).
- ³T. Valet and A. Fert, Phys. Rev. B **48**, 7099 (1993).
- ⁴V. A. Oboznov, V. V. Bol'ginov, A. K. Feofanov, V. V. Ryazanov, and A. I. Buzdin, Phys. Rev. Lett. **96**, 197003 (2006).
- ⁵A. F. Volkov, F. S. Bergeret, and K. B. Efetov, Phys. Rev. Lett. **90**, 117006 (2003).
- ⁶S. D. Steenwyk, S. Y. Hsu, R. Loloee, J. Bass, and W. P. Pratt, Jr., J. Magn. Magn. Mater. **170**, L1 (1997).
- ⁷A. C. Reilly, W. Park, R. Slater, B. Ouaglal, R. Loloee, W. P. Pratt, Jr., and J. Bass, J. Magn. Magn. Mater. **195**, L269 (1999).
- ⁸L. Piraux, S. Dubois, A. Fert, and L. Belliard, Eur. Phys. J. B **4**, 413 (1998).
- ⁹I. C. Moraru, W. P. Pratt, Jr., and N. O. Birge, Phys. Rev. Lett. **96**, 037004 (2006).
- ¹⁰J. Bass and W. P. Pratt, Jr., J. Magn. Magn. Mater. **200**, 274 (1999), and references therein.
- ¹¹S. F. Lee, Q. Yang, P. Holody, R. Loloee, J. H. Hetherington, S. Mahmood, B. Ikegami, K. Vigen, L. L. Henry, P. A. Schroeder, W. P. Pratt, Jr., and J. Bass, Phys. Rev. B **52**, 15426 (1995).
- ¹²Data from samples with thicker Ni layers had unusually small values of ΔR and large coercive fields for the free layer approaching the pinning field of the Py layer. These observations indicate that the AP state was poorly formed; hence these data were discarded. Superconducting quantum interference device magnetometry measurements of isolated Ni films of thicknesses 80 and 200 nm show low remanent magnetization and large saturation field. The behavior of the latter is similar to that seen in epitaxial (100) Ni films (Ref. 13), which was interpreted as evidence of out-of-plane magnetization.
- ¹³M. A. Marioni, N. Pilet, T. V. Ashworth, R. C. O'Handley, and H. J. Hug, Phys. Rev. Lett. **97**, 027201 (2006).
- ¹⁴M. D. Stiles and D. R. Penn, Phys. Rev. B **61**, 3200 (2000).
- ¹⁵C. Fierz, S. F. Lee, J. Bass, W. P. Pratt, Jr., and P. A. Schroeder, J. Phys.: Condens. Matter **2**, 9701 (1990).
- ¹⁶J. A. Borchers, J. A. Dura, J. Unguris, D. Tulchinsky, M. H. Kelley, C. F. Majkrzak, S. Y. Hsu, R. Loloee, W. P. Pratt, Jr., and J. Bass, Phys. Rev. Lett. **82**, 2796 (1999).